

Synthesis of some substituted pyrazinopyridoindoles and 3D QSAR studies along with related compounds: Piperazines, piperidines, pyrazinoisoquinolines, and diphenhydramine, and its semi-rigid analogs as antihistamines (H₁)

Mridula Saxena, Stuti Gaur, Philip Prathipati and Anil K. Saxena*

Medicinal and Process Chemistry Division, Central Drug Research Institute, Lucknow 226001, India

Received 20 May 2006; revised 8 September 2006; accepted 9 September 2006

Available online 28 September 2006

Abstract—3D QSAR studies on the title compounds led to the development of a model with three biophoric sites and six secondary sites viz. H-acceptor (ACC), H-donor (DON), heteroatom (presence), hydrophobic (hydrophobicity), steric (refractivity), and a ring (presence) along with total hydrophobicity and total refractivity as global properties. The model predicted the test set of compounds reasonably well. Three of the five newly synthesized 2-substituted octahydropyrazinopyridoindoles have shown potent antihistaminic H₁ activity with less toxicity and sedation potential.

© 2006 Elsevier Ltd. All rights reserved.

1. Introduction

Histamine¹ is an intercellular chemical messenger and plays a critical role in several diverse physiological processes. Four human G-protein coupled histamine receptor subtypes (H₁₋₄)² are currently recognized to mediate various actions of the monoamine histamine. These include smooth muscle contraction, inflammatory response, gastric acid secretion, and mediation of neurotransmitter release in central nervous system. There has been a tremendous increase in knowledge about the role of histamine through specific activation or blockade of these receptor subtypes both in physiology and pathology. Among the four subtypes, the histamine H₁ receptor has been an attractive target for drug discovery for several years and H₁ receptor antagonists³ have proved to be effective therapeutic agents for respiratory distress, thus contributing to an important class of drugs today.

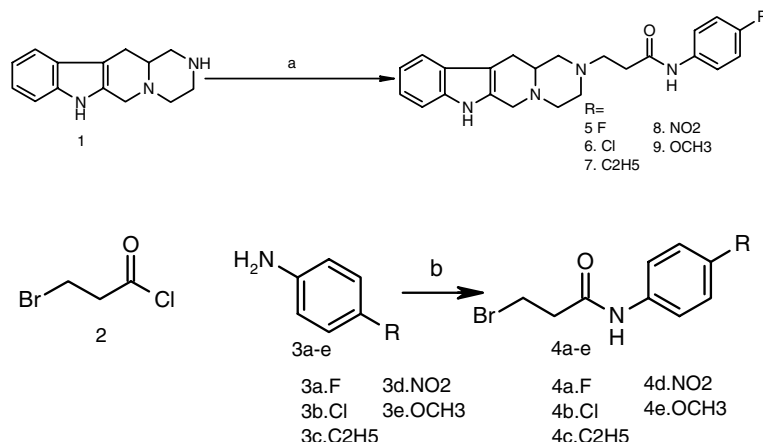
In our earlier ligand-based QSAR and pharmacophore study, models were developed by classical techniques like Hansch's physicochemical methods and HASL.⁴⁻⁷

The QSAR studies in 2-β-arylaminoethyl-1,2,3,4,6,7,12,12a-octahydropyrazino(2',1':6,1)pyrido(3,4-b)indoles⁴ emphasized the importance of hydrophobicity of the substituent at *ortho* and *para*-position and bulk at the *ortho* position of the aromatic ring of the arylaminoethyl side-chain, which contribute positively to increase in activity. Further, in view of the similarity in terms of positive steric effect of substitution at the phenyl ring of these molecules as of diphenhydramine, it was suggested that these molecules bind to the H₁ receptor in a folded conformation whereby the phenyl and indole rings of these molecules occupy similar positions as the two phenyl rings of diphenhydramine.⁶

Keeping in view that the same structural variations in a common substructure present in different prototypes should show similar change in activity (because of its association with the complementary subsites at the receptor) the above model was further explored. Thus different types of compounds viz. 1-[(arylamino)ethyl]-4-benzyl-piperazines and -piperidines, 1-{2-[(arylamino)carbonyl]ethyl}-4-benzyl-piperazines and -piperidines, 2-[(arylamino)carbonyl]ethyl-1,2,3,4,6,7,12,12a-octahydropyrazino[2',1':6,1]pyrido[3,4-b]indoles, and {2-[(arylamino)carbonyl]ethyl}-1,2,3,4,6,11,11a-hexahydro-2H-pyrazino[1,2-b]isoquinolines were studied to see the effect of substitution on the phenyl ring of the aryl part on antihistaminic (H₁) activity.⁵ The similar slope value

Keywords: QSAR; H₁-antihistamine; Apex-3D; Catalyst.

* Corresponding author. Tel.: +91 522 2612411 18; fax: +91 522 2623405; e-mail: anilsak@gmail.com



Scheme 1. Reagents and conditions: (a) β-bromo-N-arylpropionamide, DMF, 60 °C, K₂CO₃, NaI (corresponding *para*-substituted β-bromo-N-arylpropionamide); (b) THF, TEA, 0 °C.

(0.304(±0.060)) associated with π in QSARs in different prototypes suggested that all the compounds appear to act on a common receptor and the essential structural requirements for the molecules to exhibit H₁ antihistaminic activity are the presence of substructures which can interact at the proposed four subsites.⁶ These studies further indicated that the application and predictive value of classical QSAR (physicochemical approach) are not limited to same prototypes. The classical QSAR can be used for the mapping of receptor sites if the common substructure competing for the same receptor sites has been identified in different prototypes.

In order to further validate these results through advanced molecular modeling techniques, the HASL approach has been used to identify the pharmacophore for H₁ receptor antagonists using the above compounds and some semi-rigid analogs of diphenhydramine, benzylhydramine, and phenbenzamine.⁷⁻⁹ These studies were among the first applications of the HASL approach, which reinforced the importance of major sites for the interaction of the tertiary nitrogen and aromatic rings.

The above knowledge has been used for the validation and improvement of our model using advanced softwares like Catalyst¹⁰ and APEX-3D.¹¹⁻¹⁶ The APEX-3D expert system has a limitation in fast generation of conformations for identifying the suitable conformation for activity while the CATALYST software is relatively poor in generating good predictive 3D QSAR models than APEX-3D. Hence an integrated approach using both expert systems has been applied to identify the 3D pharmacophore for the above-mentioned antihistamines H₁ and some newly synthesized 2-[β-(N-aryl)propionamido]-1,2,3,4,6,7,8,12,12a-octahydro-pyrazino[2',1':6,1]pyrido[3,4-b]indoles (5-9).

2. Chemistry

The 2-[β-(N-4-substitutedphenyl)propionamido]-1,2,3,4,6,7,8,12,12a-octahydro-pyrazino[2',1':6,1]pyrido[3,4-

b]indoles (5-9) were synthesized by the condensation of the intermediate 1,2,3,4,6,7,8,12,12a-octahydro-pyrazino[2',1':6,1]pyrido[3,4-*b*]indole¹⁷ with appropriate β-bromo-N-arylpropionamides in presence of triethylamine, essentially according to the method described in the literature for similar compounds⁶ (Scheme 1). The required β-bromo-N-arylpropionamides (4a-e) were synthesized by the condensation of β-bromopropionyl chloride with an appropriate arylamine in presence of triethylamine (Scheme 1).

3. Pharmacology

The antihistamine (H₁) activity of compounds 5-9 was measured on the isolated terminal part of the guinea pig ileum (5.0 cm long) suspended in an organ bath containing aerated Tyrode solution (20 ml) at 35 °C and spasm of the ileum was induced by 3 × 10⁻⁸ g/mL of histamines. The percentage of inhibition was plotted against different concentrations of the compound and the concentration causing 50% inhibition (IC₅₀) was calculated (Table 1).

The compounds 5, 6, and 7 showed promising activity among the newly synthesized compounds. Hence these compounds were also evaluated for other pharmacological effects including acute toxicity, gross observational effects, antagonism to amphetamine hyperactivity, and toxicity in aggregated mice. Electroshock seizures were studied in male mice by the standard method.¹⁷⁻¹⁹ The effect on blood pressure was also studied in anesthetized cats by administering 2.5 μmol/kg iv.²⁰

4. Molecular modeling

A 3D biophoric model was developed for H₁ receptor antagonists using the newly synthesized 2-[β-(N-aryl)propionamido]-1,2,3,4,6,7,8,12,12a-octahydro-pyrazino[2',1':6,1]pyrido[3,4-*b*]indoles (5-9) (Table 1) and the compounds 10-49 (Table 2) reported in our previous papers.⁵⁻⁷ All the 45 molecules were aligned using

Table 1. Antihistaminic (H_1) activities for compounds 5–9

Compound	Antihistaminic activity				ALD ₅₀ mg/kg ip (mice)	Gross effect at 0.2 LD ₅₀ dose mg/kg ip (mice) ^a
	IC ₅₀ μ mol/L	–logIC ₅₀ observed	–logIC ₅₀ calculated	–logIC ₅₀ predicted		
5	0.35 \pm 0.06	0.46	0.69	0.72	1000	Stimulation
6	0.2 \pm 0.03	0.7	0.62	0.59	1000	Stimulation
7	0.19 \pm 0.02	0.72	0.38	0.32	1000	Depression
8	2.6 \pm 0.4	–0.41	–0.34	–0.33	>1000	Depression
9	2.27 \pm 0.07	0.57	0.28	0.25	>1000	Depression
Mepyramine	0.006 (1.6 μ g/ml)				62	

^a Depressant implies reduction in spontaneous motoractivity, ataxia, and loss of writhing reflex; Stimulation implies increased active straup phenomenon, preconvulsiveness, and convulsions.

CATALYST¹⁰ molecular modeling software and the resulting alignment was used in generating the 3D biophoric model by Apex 3D software.¹¹

The 3D structures of the training set of the 45 molecules (Tables 1 and 2) with antihistaminic activities distributed over a range of 3 orders of magnitude were built and optimized for their geometry using the CHARMM forcefield²¹ in the usual way and the conformations were generated using the maximum limit of 250 conformations within a 20 kcal cut-off by applying the poling algorithm²² as implemented in the Catalyst molecular modeling software version 4.5 running on SGI O2 workstation. The common feature hypothesis²³ was developed using the default parameters and taking diphenhydramine (compound 45, one of the most active molecules) as a template onto which the rest of the 43 H_1 antagonists were superimposed using the Catalyst HipHop module. The common feature hypothesis was produced by generating alignments of common features, which included aromatic rings and positive ionizable groups.

The best alignments generated from common feature alignment (HipHop) were subjected to different computational chemistry programs including MOPAC 6.0 version (MNDO Hamiltonian)²³ for the calculation of different physicochemical and quantum chemical parameters: atomic charge, π -population, H-donor and acceptor index, HOMO, LUMO, hydrophobicity, and molar refractivity based on atomic contributions, which were then used by the APEX-3D expert system running on a SGI Indy workstation, for the automated identification of pharmacophore and 3D QSAR model building. The training set compounds with antihistaminic activities were classified into the following three classes: (i) very active (≥ 2.40), (ii) active (< 2.40 and ≥ -0.85), and (iii) less active (> -0.85).

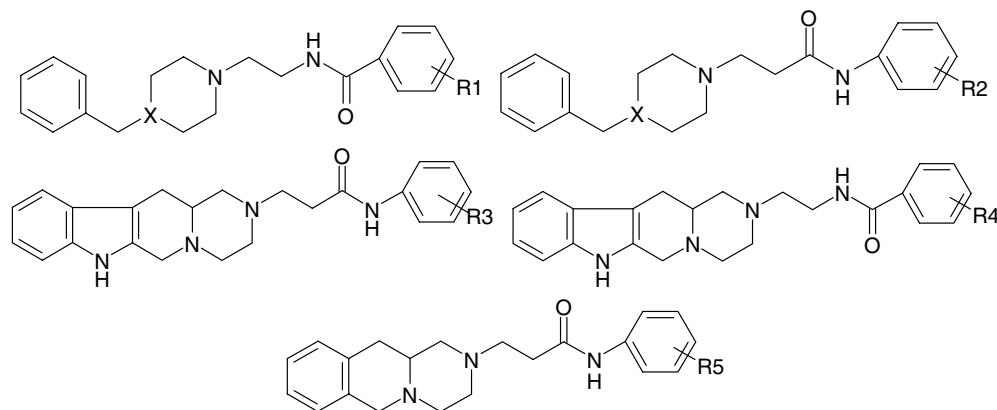
5. Results and discussion

HipHop provides feature-based alignment of a collection of compounds without considering activity. Among the eight generated hypotheses, six hypotheses contain two-three features with the ranking scores ranging from 80.3518 to 25.2954. These six hypotheses consist of the same common-feature functions of two ring aromatic and one positive ionizable (RRP) fea-

ture. The second group of two hypotheses is characterized by two ring aromatic (RR) features. The ring aromatic feature may represent the aromatic rings involved in π – π interactions and the positive ionizable group represents the charged nitrogen, which may be involved in electrostatic interaction with an acidic residue on the receptor. The latter is known to be an important interaction between a ligand and the receptors of G-protein coupled receptor (GPCR) family to which histamine H_1 receptor belongs.

The ranking of hypotheses is based on the portion of training set members that fit the proposed pharmacophore and the rarity of the pharmacophore. The higher the ranking, it is less likely that the molecules fit the hypothesis by a chance correlation. The highest ranking hypothesis of each group is shown in (Table 3) and the active molecule is shown to map well to the highest ranking hypothesis 1 (Fig. 1) representing a pharmacophore which is an essential three-dimensional arrangement of functional groups that a molecule must possess for its recognition at the active site. This pharmacophore model has two ring aromatic features and a positive ionizable group as proposed in our earlier studies and in the pharmacophore model proposed by Ter Laak et al.²⁴ However, it differs from the earlier proposed model in that it has no feature to account for the anionic site and in terms of the inter-feature distances proposed in the model of Ter Laak et al. (inter-feature distances in this model: R1-P is 5.247, R1-R2 is 4.971, and R2-P is 6.88, while in the model proposed by Ter Laak et al.²⁵ R1-P is 8.73, R1-R2 is 4.79, and R2-P is 9.10). This inconsistency in the inter-feature distance may be because of the different chemical classes of molecules analyzed in each of these models. Further the works of Wieland et al.²⁶ on the active antagonistic site region of histamine H_1 receptor prove that, one of the aromatic rings of the antagonists forms favorable aromatic π – π stacking interactions with Phe 433 and Phe 436, the other ring establishes aromatic π – π stacking with Trp 167, in addition the nitrogen establishes a salt bridge interaction with ASP 116. While aromatic interactions are accounted for the ring aromatic features of the hypotheses, the ionic salt bridge interaction is accounted for the positive ionizable feature.

Among several 3D biophoric models developed by the APEX-3D expert system using the alignments of common feature hypothesis 1 for all the molecules of the

Table 2. Molecules of the training set (activity IC₅₀ μmol/L)

Compound	X	R1	R2	R3	R4	R5	IC ₅₀ μmol/L ^a	-logIC ₅₀		
								Obs. ^b	Calc. ^c	Pred. ^d
10	N	2-I	—	—	—	—	0.345	0.46	0.12	0.1
11	N	2-Br	—	—	—	—	0.421	0.38	0.35	0.35
12	N	2-Cl	—	—	—	—	0.696	0.16	0.12	0.12
13	N	2-NO ₂	—	—	—	—	1.318	-0.12	0.12	0.13
14	N	2-CH ₃	—	—	—	—	7.12	-0.85	0.12	0.18
15	N	H	—	—	—	—	6.94	-0.84	-0.51	-0.37
16	CH	H	—	—	—	—	1.548	-0.19	-0.26	-0.27
17	CH	2-Br	—	—	—	—	0.661	0.18	-0.01	-0.08
18	CH	2-Cl	—	—	—	—	0.799	0.1	-0.01	-0.05
19	CH	2-CH ₃	—	—	—	—	1.071	-0.03	-0.17	-0.22
20	CH	—	2-C ₂ H ₅	—	—	—	0.477	0.32	-0.17	-0.31
21	CH	—	2-Cl	—	—	—	0.561	0.25	0.28	0.29
22	CH	—	2-F	—	—	—	0.832	0.08	-0.41	-0.54
23	CH	—	2-OCH ₃	—	—	—	0.963	0.02	0.12	0.13
24	CH	—	H	—	—	—	1.513	-0.18	0.6	0.68
25	N	—	2-C ₂ H ₅	—	—	—	0.778	0.11	-0.18	-0.22
26	N	—	2-Cl	—	—	—	0.836	0.08	0.15	0.16
27	N	—	2-F	—	—	—	1.318	-0.12	0.15	0.2
28	N	—	2-NO ₂	—	—	—	1.701	-0.23	-0.18	-0.18
29	N	—	H	—	—	—	2.167	-0.34	-0.34	-0.35
30	—	—	—	H	—	—	1.604	-0.2	-0.38	-0.53
31	—	—	—	2-C ₂ H ₅	—	—	0.634	0.2	0.55	0.62
32	—	—	—	2-Cl	—	—	0.979	0.01	-0.1	-0.11
33	—	—	—	2-F	—	—	0.776	0.11	0.24	0.27
34	—	—	—	2-NO ₂	—	—	1.738	-0.24	0.52	0.6
35	—	—	—	—	H	—	0.537	0.27	-0.13	-0.2
36	—	—	—	—	2-Cl	—	0.206	0.69	0.52	0.51
37	—	—	—	—	2-CH ₃	—	0.282	0.55	0.6	0.61
38	—	—	—	—	2-OCH ₃	—	0.364	0.44	0.52	0.51
39	—	—	—	—	2-NO ₂	—	0.380	0.42	0.21	0.15
40	—	—	—	—	2-NH ₂	—	0.930	0.03	0.21	0.15
41	—	—	—	—	—	H	1.342	-0.13	0.12	0.13
42	—	—	—	—	—	2-C ₂ H ₅	0.525	0.28	0.12	0.13
43	—	—	—	—	—	2-Cl	0.677	0.17	0.12	0.12
44	—	—	—	—	—	2-NO ₂	1.316	-0.12	0.01	0.03
45							0.0039	2.41	2.04	1.78

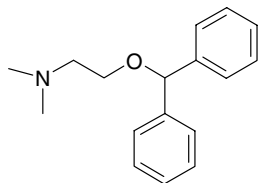
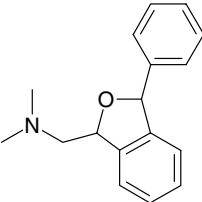
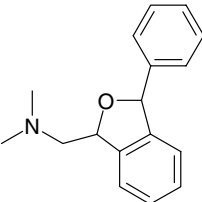
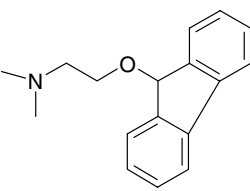
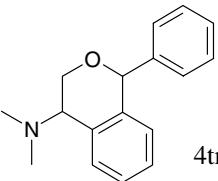


Table 2 (continued)

Compound	X	R1	R2	R3	R4	R5	IC ₅₀ μmol/L ^a	-log IC ₅₀		
								Obs. ^b	Calc. ^c	Pred. ^d
46			3cis				0.0039	2.41	—	—
47			2trans				0.0039	2.41	2.26	2.09
48							0.039	1.410	—	—
49			4trans				0.513	0.290	—	—

^aInhibitory concentration for 50% block of histamine.

^bObserved.

^cCalculated.

^dPredicted.

Table 3. Hypothesis obtained through Catalyst

S. No.	Hypothesis ^a	Rank	DH ^b	PH ^c
1	RRP	80.3518	111111111111	000000000000
2	RR	25.2954	111111111111	000000000000

^aR, ring aromatic; P, positive ionizable.

^bDH, direct hit, all the features of the hypothesis are mapped. Direct hit = 1, means yes and direct hit = 0, means no.

^cPH, partial hit, partial mapping of the hypothesis.

training set, none of the biophores could map to all the molecules of the training set. So a model which included maximum number of compounds (42 out of 45) was selected based on the following criteria; maximum number of compounds, correlation coefficient $r^2 > 0.7$, the difference between RMSA and RMSP < 0.03 (a measure of cross-validation), chance ≤ 0.1 , no. of variables < 7 , and compounds > 41 (Table 4). The exclusion of the three compounds (46, 48, and 49) is due to their ability to map to the three biophoric sites of the model. This may be due to the misfitting of the spatial geometry of essential atom types (biophoric sites) which is associated

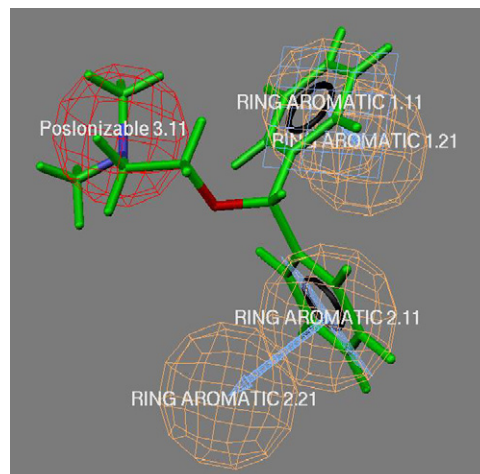
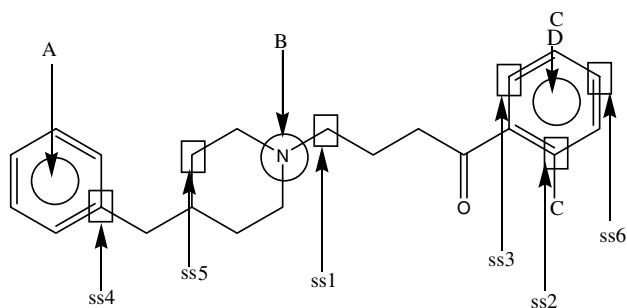
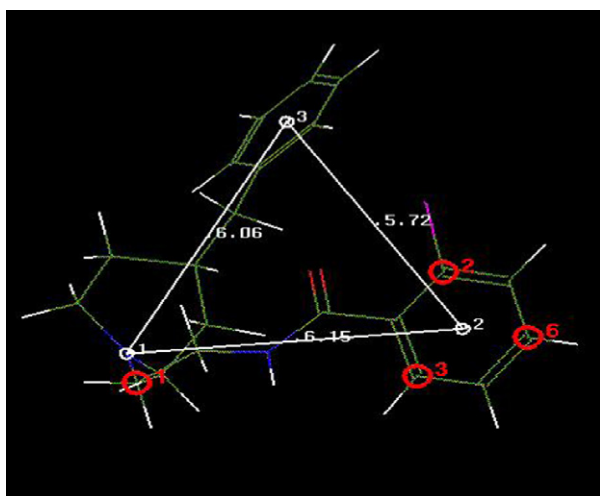
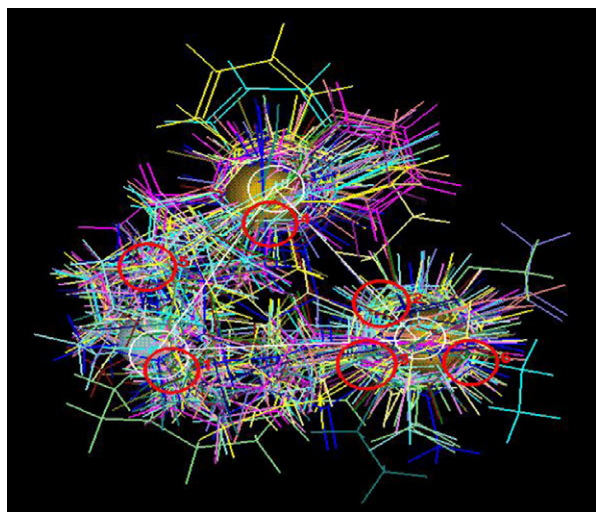


Figure 1. Mapping of compound 45 to hypothesis 1.

with the introduced semi-rigidity in the diphenhydramine molecule (45). The model is highly significant and does not suffer from overfitting as evidenced by a

Table 4. 3D QSAR model describing correlation and statistical reliability for H1 antihistaminic activity

Model no.	RMSA	RMSP	R2	Chance	Size	Match	Variable	No. of compounds
1	0.348	0.376	0.73	0.1	3	0.22	6	42

**Figure 2.** Representation of biophoric (O) and secondary sites (□).**Figure 3.** Compound 18 showing the distances between the biophoric sites (white circles). The distances are given in angstrom units.**Figure 4.** Superimposition of the 42 molecules for pictorial representation of biophoric sites (solid spheres) and secondary sites (red circles).

small difference (0.028) between root mean squared approximation (RMSA) and leave-one-out prediction (RMSP), as a big difference in RMSA and RMSP is caused by influential compounds that are overfitted by the multiple regression and are poorly predicted when not included in the training set.

This model comprised three biophoric features (Figs. 2–4), corresponding to the earlier suggested sites ABD.⁶ The biophoric sites A and D in terms of 6π electrons provided by either of the aromatic rings of the six prototypes (1-[aroylamino]ethyl]-4-benzyl-piperazines and -piperidines, 1-{2-[arylamino]-carbonyl]ethyl}-4-benzyl-piperazines and -piperidines, 2-[arylamino]carbonyl]ethyl-1,

Table 5. Secondary site parameters: hydrophobicity (ss 1–4) and refractivity (ss 5–6) for the training set

Compound	ss1	ss2	ss3	ss4	ss5	ss6
5	—	0	−0.1	—	—	3.45
6	—	—	−0.1	0.15	—	—
7	−0.85	—	—	—	2.5	3.9
8	−0.85	—	—	0	3.5	—
9	—	—	—	—	—	—
10	—	—	—	—	—	—
11	−0.85	—	0.15	—	—	—
12	—	—	—	—	—	—
13	—	—	—	—	—	—
14	—	—	—	—	—	—
15	—	0	0.15	0	2.9	3.45
16	—	—	—	0	2.9	3.45
17	−0.85	—	0	—	—	3.45
18	−0.85	—	0	—	—	3.45
19	—	—	0.15	0.15	2.9	3.45
20	—	0	−0.1	0.15	2.9	—
21	—	—	−0.1	—	—	—
22	−0.85	—	—	—	—	—
23	—	—	0	—	—	—
24	−0.85	0	—	—	—	—
25	−0.85	—	—	—	2.9	—
26	−0.85	—	—	0.15	2.9	—
27	−0.85	—	—	—	2.9	—
28	−0.85	0	0	—	3.5	—
29	—	—	−0.1	−0.3	—	—
30	−0.85	—	—	0.15	2	0.9
31	—	0	−0.1	—	2.9	3.45
32	—	—	—	—	—	—
33	—	0	—	—	—	3.45
34	—	—	0.15	—	—	—
35	—	0	—	—	—	—
36	—	—	—	—	—	—
37	—	0	—	—	—	—
38	—	—	0.15	0.15	—	—
39	—	—	—	—	—	—
40	—	—	—	—	—	—
41	—	—	—	—	—	—
42	—	—	—	—	—	—
43	—	—	—	—	—	—
44	—	—	−0.1	—	2.5	3.45
45	−1.1	0	—	—	—	—
47	—	—	—	—	—	—

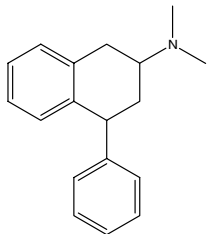
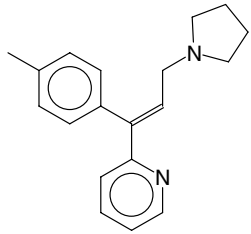
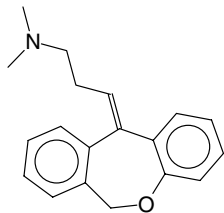
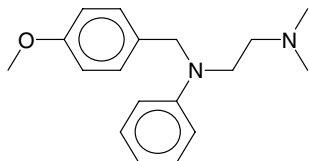
2,3,4,6,7,12,12a-octahydropyrazino[2',1':6,1]pyrido[3,4-b]indoles and {2-[(arylamino)carbonyl]ethyl}-1,2,3,4,6,11,11a-hexahydro-2*H*-pyrazino[1,2-*b*]isoquinolines as well as the diphenhydramine and its semi-rigid analogs) correspond to π - π interactions and site B corresponds to the protonable tertiary nitrogen provided by tertiary amino function present in all the molecules in terms of π -population (0.164 ± 0.009) for electrostatic interactions with the receptor with a particular spatial disposition; the mean inter-atomic distances of three biophoric sites A, B, D being A–D (5.585 ± 0.398), A–B (6.2181 ± 0.421), and B–D (5.5013 ± 0.488).

In order to understand the interactions and to identify the secondary sites for explaining the variation in anti-histaminic activity, the 3D-QSAR model was

derived using this biophore as a template for superimposition and the antihistaminic activity ($-\log IC_{50}$) as a dependent variable and biophoric center properties (π -population, charge, HOMO, LUMO, ACC_01, Don_01, hydrophobicity, and refractivity), global properties (total hydrophobicity and total refractivity), secondary sites [H-acceptor (ACC), H-donor (DON), heteroatom (presence), hydrophobic (hydrophobicity), steric (refractivity), and ring (presence)] as independent variables with the occupancy set at 12, site radius at 0.60, sensitivity at 1.0, and randomization value at 100.

The derived 3D QSAR model Eq. 1 correlated the antihistaminic activity with secondary site parameters hydrophobicity, at secondary site ss1 [6.269 ± 0.411],

Table 6. Observed versus predicted activity of test compounds

Compound	Test set compounds	Antihistaminic activity H1	
		Predicted activity ^a $-\log IC_{50}$	Observed activity $K_{1,K0.5}$ ^b (nM)
50		1.640	1.070
51		0.120	0.46
52		0.120	0.16
53		0.450	0.53

^a Predicted using Eq. 1.

^b As reported in the literature,²⁷ $K_{0.5}$ is a competition binding assay endpoint and is calculated from IC_{50} value using the Cheng–Prusoff equation, $K_{0.5} = IC_{50}/(1 + L/K_D)$.

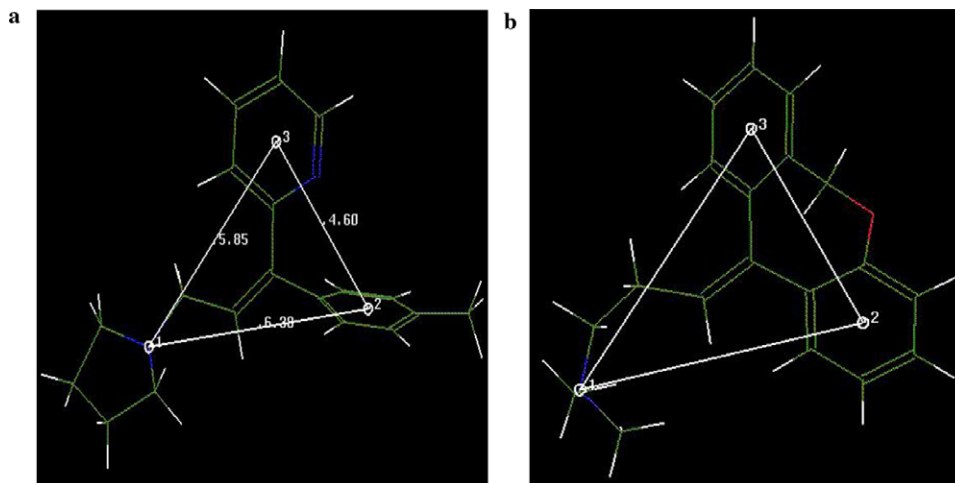


Figure 5. (a) Compound **51** mapping to the biophore produced by APEX-3D. (b) Compound **52** mapping to the biophore produced by APEX-3D.

(1.511 ± 0.166), (6.085 ± 0.37) $^{\circ}$ A from the biophoric sites ABD, respectively], secondary site ss2 [(1.561 ± 0.581), (5.464 ± 0.373), (4.014 ± 0.814) $^{\circ}$ A from the biophoric sites ABD, respectively], secondary site ss3 [(2.08 ± 1.611), (5.119 ± 0.479), (4.993 ± 1.606) $^{\circ}$ A from the biophoric sites ABD, respectively], secondary site ss4 [(4.797 ± 1.067), (4.717 ± 0.274), (1.526 ± 0.875) $^{\circ}$ A from the biophoric sites ABD, respectively], and steric effect in terms of refractivity, at secondary site ss5 [(6.51 ± 0.915), (4.717 ± 0.274), (4.234 ± 0.927) $^{\circ}$ A from the biophoric sites ABD, respectively] and secondary site ss6 [(1.405 ± 0.006), (2.663 ± 0.231), (6.885 ± 0.370) $^{\circ}$ A from the biophoric sites ABD, respectively].

$$\begin{aligned} \log(\text{IC}_{50}) = & -0.564(\pm 0.140) \\ & \times [\text{Hydrophobicity at ss1}] \\ & + 10.097(\pm 1.287) \\ & \times (\text{Hydrophobicity at ss2}) \\ & - 1.638(\pm 0.752) \\ & \times [\text{Hydrophobicity at ss3}] \\ & + 2.209(\pm 0.738) \\ & \times [\text{Hydrophobicity at ss4}] \\ & - 0.270(\pm 0.044)[\text{Refractivity at ss5}] \\ & + 0.117(\pm 0.034)[\text{Refractivity at ss6}] \\ & + 0.12 \end{aligned} \quad (1)$$

$$n = 42, R = 0.855, F_{6,36} = 16.376, Q = 0.794, S = 0.335$$

The secondary sites ss1, ss3, and ss5 in terms of hydrophobicity and refractivity contribute negatively while secondary sites ss2 corresponding to the hydrophobicity at the *ortho* position of the side-chain phenyl group, and ss4 and ss6 in terms of hydrophobicity and refractivity, respectively, contribute positively to the activity. The values of hydrophobicity and refractivity parameters at these sites are shown in Table 5. Equation 1 well describes the observed antihistaminic activity with good correlation coefficient value ($R = 0.86$), low standard deviation ($S = 0.335$), and is of high statistical signifi-

cance $>99\%$ ($F_{6,36 \times 0.001} = 5.39$; $F_{6,36} = 16.38$) and also shows good leave-one-out cross-validation with Q -value of 0.794 as well low RMSA and RMSP as discussed earlier. Further this is also evident by the good correspondence between the observed, calculated, and (LOO) predicted values (Table 1).

For the validation of the above 3D QSAR model an external test set of four compounds devoid of asymmetric center viz. (\pm)-*trans*-1-Phenyl-3-(dimethylamino)-1,2,3,4-tetrahydronaphthalene (**50**), triprolidine (**51**), doxepin (**52**), and mepyramine (**53**) was used from the reported data.²⁷ The model predicted the activity of these four compounds as $-\log \text{IC}_{50}$ values corresponding to the training sets' IC_{50} values (Table 6, four compounds were in terms of $K_{0.5}$ (nM)), the values as such may not be compared, nevertheless a very good correlation ($R^2 = 0.8904$) was observed between the observed and predicted values and also map well to the biophoric sites of the model (Fig. 5a and b).

Among the five new compounds (**5–9**) synthesized, the compounds **5**, **6**, and **7** showed relatively high activity and low toxicity among the 2-[β -(*N*-4-substituted-phenyl)propionamido]-1,2,3,4,6,7,8,12,12a-octahydro-pyrazino[2',1':6,1]pyrido[3,4-*b*]indole. Though they were less active than mepyramine, the compounds **5**, and **6** were stimulant in gross behavior and also did not show significant hypotensive action in cats ($>20\%$ B.P fall for >5 min), thus indicating that they may have no sedative potential.

6. Conclusion

The above studies substantiate the findings of our earlier QSAR studies where the major limitation was non-inclusion of diverse types of molecules into one model. The 3D QSAR model described here using an integrated approach of taking the pharmacophore mapping through the application of CATALYST software and 3D QSAR model development from Apex modeling not only well describes the variance in activity of the training set but also maps and explains the estimated

activity of the test set molecules reasonably well. Most of the published 3D QSAR models on antihistamines are CoMFA based, which are relatively less versatile in terms of predicting the activity of different types of molecules. The present model may be useful in designing and optimizing non-classical antihistamines H₁, which may also be non-sedative.

7. Experimental

Microanalysis was performed on a Carlo Erba Analyzer and compounds were analyzed for nitrogen. Melting points were determined on an electrically heated mp apparatus using a silicon oil bath. The compounds were routinely checked for purity by TLC on silica gel plates and their structures were verified by their IR spectra measured on Perkin-FTIR model PC spectrophotometer, FAB mass spectra were recorded on JEOL SX 102/DA-6000 mass using Argon/Xenon (6 KV, 10 MA) as the FAB gas and ¹H NMR spectra recorded on a Bruker spectrometer (200 MHz) with a multinuclear inverse probehead with gradient at room temperature (298 K) using CDCl₃ or DMSO-*d*₆ or CD₃OD as solvent and tetramethylsilane (TMS) as internal standard.

7.1. General procedure for the synthesis of 2-[β-(*N*-4-substituted-phenyl)propionamidol]-1,2,3,4,6,7,8,12,12a-octahydropyrazino[2',1':6,1]pyrido[3,4-*b*]indoles

The appropriate β-bromo-*N*-(4-substituted phenyl)propionamide (0.0051 mol) in dry DMF (2 ml) was added to a suspension of dl-1,2,3,4,6,7,8,12,12a-octahydropyrazino[2',1':6,1]pyrido[3,4-*b*]indole (**5**) (0.005 mol) and Na₂CO₃ (0.0025 mol) in dry DMF (5 ml), and the reaction mixture was stirred for 36 h at 60 °C. It was cooled to 30 °C, diluted with water (20 ml), and extracted with chloroform (3 × 10 ml). The combined chloroform extracts were washed with water (2 × 5 ml), dried over Na₂SO₄, and concentrated under reduced pressure to give the corresponding title compounds which were purified by column chromatography over silica gel using methanol (1–2%) in chloroform as elutant.

7.2. 2-[β-(*N*-4-Fluorophenyl)propionamidol]-1,2,3,4,6,7,8,12,12a-octahydro-pyrazino[2',1':6,1]pyrido[3,4-*b*]indole (**5**)

Mp 102 °C; yield: 93.45%; IR (KBr) cm⁻¹: 3298, 3065, 2929, 2825, 1663, 744; ¹H NMR (CDCl₃) δ: 2.29–3.23 (m, 13H); 3.54–3.61 (m, 1H); 3.99–4.06 (d, 1H, *J* = 14); 6.94–7.53 (m, 8H); 7.78 (s, 1H); 10.83 (s, 1H); FAB-MS = 393M⁺; Anal. Calcd for C₂₃H₂₄ON₄F: N, 14.29. Found: N, 14.28. C₂₃H₂₅FN₄O.

7.3. 2-[β-(*N*-4-Chlorophenyl)propionamidol]-1,2,3,4,6,7,8,12,12a-octahydro-pyrazino[2',1':6,1]pyrido[3,4-*b*]indole (**6**)

Mp 100 °C; yield: 98.13%; IR (KBr) cm⁻¹: 3278, 2931, 2825, 1662, 743; ¹H NMR (CDCl₃) δ: 2.29–2.90 (m, 11H); 3.05–3.23 (m, 2H); 3.55–3.62 (m, 1H); 3.99–4.07 (m, 1H); 7.09–7.51 (m, 8H); 7.78 (s, 1H); 10.99 (s, 1H);

FAB-MS = 409 M⁺; Anal. Calcd for C₂₃H₂₄ON₄Cl: N, 13.71. Found: N, 13.66. C₂₃H₂₅ClN₄O.

7.4. 2-[β-(*N*-4-Ethylphenyl)propionamidol]-1,2,3,4,6,7,8,12,12a-octahydro-pyrazino[2',1':6,1]pyrido[3,4-*b*]indole (**7**)

Mp 142 °C; yield: 85%; IR (KBr) cm⁻¹: 3250, 2930, 2823, 1660, 742; ¹H NMR (CDCl₃) δ: 1.15–1.25 (m, 3H); 2.29–2.81 (m, 13H); 3.09–3.23 (m, 2H); 3.53–3.61 (m, 1H); 3.98–4.05 (m, 1H); 7.06–7.46 (m, 8H); 7.78 (s, 1H); 10.75 (s, 1H); FAB-MS = 403 M⁺; Anal. Calcd for C₂₅H₂₉ON₄: N, 13.93. Found: N, 13.82. C₂₅H₃₀N₄O.

7.5. 2-[β-(*N*-4-Nitrophenyl)propionamidol]-1,2,3,4,6,7,8,12,12a-octahydropyrazino[2',1':6,1]pyrido[3,4-*b*]indole (**8**)

Mp 148–149 °C; yield: 80%; IR (KBr) cm⁻¹: 3397, 2930, 2829, 1665, 747; ¹H NMR (CDCl₃) δ: 2.29–3.23 (m, 13H); 3.56–3.62 (m, 1H); 4.00–4.07 (d, 1H, *J* = 14); 7.10–7.51 (m, 8H); 7.76 (s, 1H); 10.99 (s, 1H); FAB-MS = 420 M⁺; Anal. Calcd for C₂₃H₂₄O₃N₅: N, 16.71. Found: N, 16.78. C₂₃H₂₅N₅O₃.

7.6. 2-[β-(*N*-4-Methoxyphenyl)propionamidol]-1,2,3,4,6,7,8,12,12a-octahydro-pyrazino[2',1':6,1]pyrido[3,4-*b*]indole (**9**)

Mp 175 °C; yield: 28.30%; IR (KBr) cm⁻¹: 3412, 3334, 2824, 2362, 1660, 742; ¹H NMR (CDCl₃) δ: 2.29–2.85 (m, 11H); 3.10–3.27 (m, 2H); 3.58–3.62 (m, 1H); 3.77 (s, 3H); 4.01–4.11 (m, 1H); 7.16–7.47 (m, 8H); 7.71 (s, 1H); 10.70 (s, 1H); FAB-MS = 405 M⁺; Anal. Calcd for C₂₄H₂₇O₂N₄: N, 13.86. Found: N, 13.72. C₂₄H₂₈N₄O₂.

Acknowledgments

The authors are thankful to the pharmacology division for providing pharmacological results, Mr. A. S. Kushwaha for his technical assistance and one of us (MS) to the DST, New Delhi, for providing financial support under WOS. This is CDRI communication number 6822.

References and notes

- Barger, G.; Dale, H. H. *J. Physiol.* **1910**, *41*, 19.
- Hofstra, C. L.; Desai, P. J.; Thurmond, R. L.; Fung-Leung, W. P. *J. Pharmacol. Exp. Ther.* **2003**, *305*, 1212.
- Zhang, M. Q.; Leurs, R.; Timmerman, H., 15th ed.. In *Berger Medicinal Chemistry and Drug Discovery*; Wolf, M. E., Ed.; John Wiley: New York, 1997; vol. 5, p 495.
- Saxena, A. K.; Dhaon, M. K.; Ram, S.; Saxena, M.; Jain, P. C.; Patnaik, G. K.; Anand, N. *Indian J. Chem.* **1983**, *22B*, 1224.
- Patnaik, G. K.; Saxena, A. K.; Saxena, M.; Srimal, R. C. *Indian J. Exp. Biol.* **1992**, *30*, 144.
- Saxena, M.; Agarwal, S. K.; Patnaik, G. K.; Saxena, A. K. *J. Med. Chem.* **1990**, *33*, 2970.

7. Saxena, A. K.; Saxena, M.; Chi, H.; Wiese, M. *Med. Chem. Res.* **1993**, *3*, 201; Gaur, S.; Prathipati, P.; Saxena, M.; Saxena, A. K. *Med. Chem. Res.* **2004**, *13*, 724.
8. Ram, S.; Saxena, A. K.; Jain (Late), P. C.; Patnaik, G. K. *Indian J. Chem.* **1984**, *B*, 1261.
9. Patnaik, G. K.; Saxena, A. K.; Dhawan, B. N. In *Aspects of Allergy and Applied Immunol*; Agarwal, M. K., Ed., 1984; Vol. 17, 75.
10. Hypotheses in Catalyst, Biosym-MSI, San Diego, CA, 1992.
11. Apex-3D, BIOSYM Technologies, Inc. San Diego, CA, USA.
12. Arokia Babu, M.; Shakya, N.; Prathipati, P.; Kaskhedikar, S. G.; Saxena, A. K. *Bioorg. Med. Chem.* **2002**, *10*, 4035.
13. Pandya, T.; Pandey, S. K.; Tiwari, M.; Chaturvedi, S. C.; Saxena, A. K. *Bioorg. Med. Chem.* **2001**, *2*, 291.
14. Pandey, S. K.; Naware, N. B.; Trivedi, P.; Saxena, A. K. *SAR QSAR Environ. Res.* **2001**, *6*, 547.
15. Kashaw, S. K.; Rathi, L.; Mishra, P.; Saxena, A. K. *Bioorg. Med. Chem. Lett.* **2003**, *15*, 2481.
16. Rathi, L.; Kashaw, S. K.; Dixit, A.; Pandey, G.; Saxena, A. K. *Bioorg. Med. Chem.* **2004**, *1*, 63.
17. Saxena, A. K.; Jain, P. C.; Dua, P. R. *J. Med. Chem.* **1973**, *16*, 560.
18. Jain, P. C.; Kapoor, V.; Anand, N.; Ahmad, A. R.; Patnaik, G. K. *J. Med. Chem.* **1967**, *10*, 812.
19. Srimal, R. C.; Dhwan, B. N. *Indian J. Pharmacol.* **1972**, *34*, 172.
20. Singh, G. B.; Srimal, R. C.; Nityanand, S.; Dhawan, B. N. *Arzneim.-Forsch* **1978**, *28*, 1087.
21. Brooks, B. R.; Bruccoleri, R. E.; Olafson, B. D.; States, D. J.; Swaminathan, S.; Karplus, A. M. *J. Comp. Chem.* **1983**, *4*, 187.
22. Smellie, A.; Teig, S. L.; Towbin, P. I. *J. Comp. Chem.* **1995**, *16*, 171.
23. Stewart, J. J. P. *J. Comput.-Aided Mol. Des.* **1990**, *4*, 101.
24. Terlaak, A. M.; Benhorst, J.; Donne-Op den Kelder, G. M.; Timmerman, H. *J. Med. Chem.* **1995**, *38*, 3351.
25. Terlaak, A. M.; Timmerman, H.; Leurs, R.; Nederkoorn, P. H.; Smit, M. J.; Donne-Op den Kelder, G. M. *J. Comput.-Aided Mol. Des.* **1995**, *9*, 319.
26. Wieland, K.; Terlaak, A. M.; Smit, M. J.; Kuhne, R.; Timmerman, H.; Leurs, R. *J. Biol. Chem.* **1999**, *42*, 22994.
27. Ehren, C.; Bucholtz, E. C.; Brown, R. L.; Tropsha, A.; Booth, R. G.; Wyrick, S. D. *J. Med. Chem.* **1999**, *42*, 3041.